Fabrication of Magnetic Co/Pt Nanodots Utilizing Filled Diblock Copolymers

A. Neumann[*,1], N. Franz[1], G. Hoffmann[1], A. Meyer[2] and H.P. Oepen[1]

[1]*Institut für Angewandte Physik, Universität Hamburg, Jungiusstraße 11, D-20355 Hamburg, Germany*

[2]*Institut für Physikalische Chemie, Universität Hamburg, Grindelalle 117, D-20146 Hamburg, Germany*

Abstract: The potential of nanosphere lithography utilizing di-block copolymers is demonstrated. The starting configuration is a single layer of micelles, filled with silica, deposited on a ferromagnetic system. After removing the organic shell the SiO_2 cores remain on the surface and are used as shadow mask for a succeeding ion milling process. It is demonstrated how the magnetic properties of the dots can be varied by tuning either the magnetic properties of the ferromagnetic layer/multilayer or the size of the cores. Dots are created that reveal ferromagnetic or superparamagnetic properties.

Keywords: Nanosphere lithography, diblock copolymers, micelle, nanodot, magnetism, ion milling, patterned media, anisotropy tuning.

INTRODUCTION

The slogan "Nano is beautiful" has been created with respect to the fascinating possibilities and rich variety of new effects that emerge due to size reduction on the nanoscale. The fields of interest cover new optical properties in nanosized semiconductors [1, 2], increased chemical activity in nanoscale catalysts [3], and one-/two- dimensional phenomenon in electrical transport and/or electronics [4-7]. Magnetic particles have attracted much attention because of their high potential in different technological fields of application. In biotechnology magnetic particles are used as contrast enhancing media in magnetic resonance imaging and as a direct addressable consistent in hypothermic treatment or drug delivery [8, 9]. A boost in the research field on magnetic nanoparticles, however, is generated due to their high potential in ultrahigh density storage media [10, 11]. The so called bit patterned media are proposed where one bit is represented by a single magnetic nanoparticle to shift the superparamagnetic limit, which is a problem in granular thin film media [12], towards smaller sizes. Magnetic nanoparticles are also important in down scaling of magnetic logic known as spintronics. Particularly in spin transfer torque devices the smaller scales reduce the current for switching and magnetization precession that generate radio frequencies [13-17]. Besides the application that is directed towards development, the investigation of the physical properties is in itself an amazing field of research.

The fabrication of magnetic nanoparticles is performed along very different routes [8, 18, 19]. A very successful approach is the synthesis using wet chemical processes. Large quantities of nanoparticles with a narrow distribution of sizes are achieved [20-23]. The limitation of this method, however, is that tuning of the magnetic properties is almost impossible. In accordance with their natural environment of fabrication (in solution) such nanoparticles are frequently and successfully used in biotechnology [24-27]. For the application in magnetic storage and spin devices a severe problem is to bring the particles on a supporting sample with the particles well aligned with regards to their crystal structure or magnetic axis [28-30]. The latter obstacle is circumvented by alternative methods that directly create the nanostructures on the supporting surface. Here, either artificial structuring of magnetic films or the so-called bottom up approach utilizing self-assembling procedures is used to generate nanoparticles at a surface. *Via* e-beam lithography perfect large arrays of almost identical particles can be fabricated which are very well adapted to the needs of storage media [31-34] although the effort of serial structuring grows tremendously when approaching the sub 50 nm limit. This bottleneck is overcome by the so-called graphoepitaxy [35, 36] which uses an artificially generated large scale pattern that serves as template for guided self-organization of organic systems which create smaller periodicities [37-39]. The arrays of smallest particle size and best homogeneity of magnetic properties have been created by this method [40]. New attempts of parallel processing were made *via* extreme ultraviolet lithography recently [41].

The direct bottom up approach is either to use self-assembling in thin film growth of magnetic systems on single crystal surfaces [42-46] or to create a nanoscaled surface morphology *via* ion milling for the deposition of magnetic material [47, 48]. Nanostructures fabricated by these methods have typically a broad distribution of sizes and the magnetic properties are fixed, determined by growth, structure and shape. For technical applications this ansatz is not from interest as it does not guarantee the tuning of geometries and magnetic properties while it is very well suited for investigation of magnetism on the nanoscale in basic research. Self-assembling of organic systems made from block copolymers is a promising route to create nanoscaled surfaces for deposition of magnetic material. The advantage over the ion milling ansatz is a higher symmetry

*Address correspondence to this author at the Institut für Angewandte Physik, Universität Hamburg, Jungiusstraße 11, D-20355 Hamburg, Germany; Tel: +49 40 42838 6371; Fax: +49 40 42838 6368;
E-mail: aneumann@physnet.uni-hamburg.de

1876-5319/12

and flexibility of the size and the geometry. The scales fit the sizes that are interesting nowadays [49-54].

Recently, the structuring of magnetic films *via* nano-sized etching masks, which are generated in a self-organization process, has gained attraction. For that purpose colloidal particles (natural lithography [55]) or polystyrene nanospheres are frequently used (nanosphere lithography [56]). On the one hand the self-assembled polystyrene spheres are covered by magnetic films and multilayers which creates separated nanodots on the top of the spheres [57] while on the other hand reactive ion etching or ion milling is used to clone the periodic structure into a magnetic thin film system [58, 59]. To tune the diameter as well as the spacing of the particles the organic spheres are shrunk in a plasma etching step before structure transfer [60-62]. A similar technique uses diblock copolymer micelles as self-assembling units which are filled with magnetic or non-magnetic material [28-30, 63-65]. Magnetic dot arrays can be directly created when magnetic core material is used and the organic shell is removed in oxygen plasma [28-30]. Alternatively, non-magnetic cores can be brought onto a magnetic film in an identical procedure. A replica of the structure is then created in the film *via* ion milling [66]; a procedure that is very close to nanosphere lithography. In this paper we report on the flexibility which is obtained by using the latter technique in which micelles with SiO_2 cores are deposited on the surface of magnetic films and multilayers.

FABRICATION PROCEDURE

All systems discussed in the following have a seed layer of platinum with a thickness of at least 4 nm. The seed layer is grown by ion beam sputtering utilizing an electron cyclotron source, which has been shown to trigger multilayers with high texture [67, 68]. The multilayers are grown *via* DC magnetron sputtering, starting with a 1 nm Pt layer grown on the seed layer and finishing with a 3 nm Pt cap layer. The thickness, roughness and texture are controlled *via* X-ray reflectometry and -diffraction. We will not comment on these properties as it is out of the scope of this paper.

The synthesis of diblock copolymers and their filling with SiO_2 is published elsewhere [69, 70]. The micelles are deposited *via* dip or spin coating. They form a close packed monomicellar layer on the multilayer film [65]. In the next step the polymer shell of the micelles is removed in oxygen plasma. The SiO_2 cores remain on top of the film. The scanning electron microscope (SEM) image (Fig. **1a**) is taken with the sample tilted by 60°. This view reveals that the well separated SiO_2 particles are spheres. The separation of the SiO_2 particles is determined by the diameter of the micelles (about 90 nm in Fig. **1**).

The structure of the particle array is transferred into the magnetic film *via* Ar ion milling at 500 eV (Fig. **2**). The sputtering takes off the film material between the particles while the SiO_2 cores protect the underlying film from being removed. The ion dose determines the amount of material which is taken off. The milling has to be stopped when the magnetic material is totally removed and before the material below the SiO_2 dots is affected. The milling process has been investigated and calibrated utilizing the evolution of the magneto-optic saturation signals of an unstructured film with the same Co/Pt layer structure [66]. A linear decrease of the Kerr signal with ion dose is found while the perpendicular easy axis of magnetization is preserved at the beginning. The latter result is important as it indicates that material is erased while the destruction of the multilayer by ion bombardment is small, evidenced by the persisting perpendicular magnetic anisotropy. This means that the stopping of the milling is not very critical as the Pt cap layer below the SiO_2 particles serves as a further protection. To determine the sputtering yields of the porous SiO_2 we have measured the ratio of the yields of silica and Pt by measuring the evaluation of dot height with atomic force microscopy (AFM) [66]. A SEM image of a magnetic dot array is shown in Fig. (**1b**). Obviously, the structure of the SiO_2 particles (Fig. **1a**) is reproduced in the multilayer film. The micrograph again is taken under an angle of 60° which reveals the three

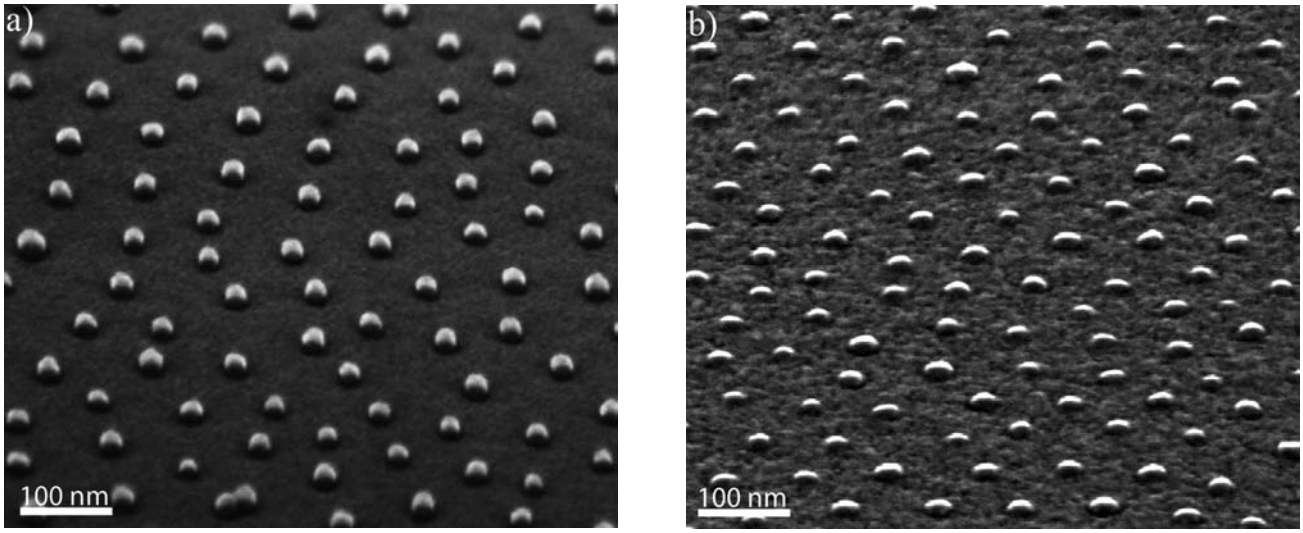

Fig. (1). SEM micrograph of SiO_2 cores (**a**) and magnetic nanodots (**b**) taken at an angle of 60°. The SiO_2 cores are spheres whereas the nanodots look more like spherical caps. The seed layer between the dots is roughened which is caused by spatially varying milling yields that depend on orientation of grains.

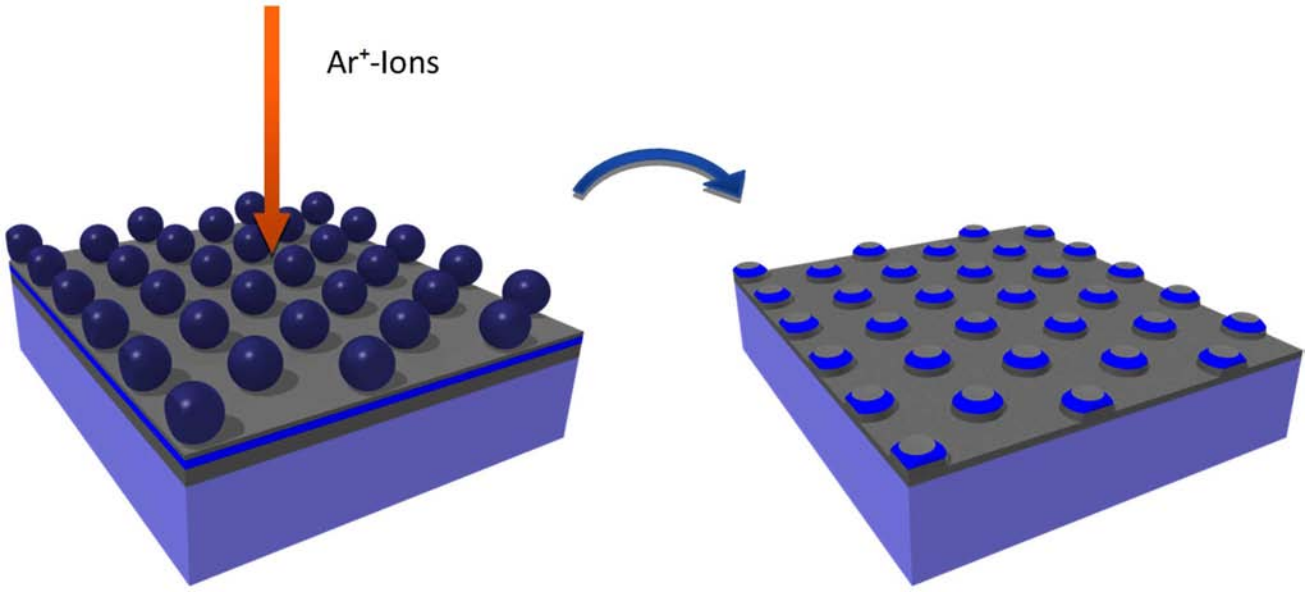

Fig. (2). Sketch of fabrication process. After removal of the polymer shell SiO_2 cores remain on the magnetic film (left-hand side). The cores are used as a shadow mask for subsequent Ar^+ ion sputtering at 500 eV. The ion milling removes the film between the SiO_2 while the material below the silica cores is preserved (right-hand side).

dimensional structure of the magnetic dots. The nanomagnets have a shape like a spherical cap. The morphology of the surface between the dots comes from a roughening of the polycrystalline seed layer due to the ion milling process. The origin is the sputtering yield that varies on the orientation of grains [71-73].

The shape of the dot that is carved into the multilayer is directly related to the shape of the particles that act as mask and depends on the ratio of the sputtering yields. A cross section of the effective shape of a spherical particle is shown in Fig. (**3a**). The amount of active material that protects the underlying film is highest in the center (thickness 2r). The thickness drops to zero within the radius of the particle (Fig. **3a**). This means that ion eroding will start from the outer rim. A profile is created and the size of the magnetic part of the dots will shrink with sputtering time (Fig. **3a**). The simulation shown in Fig. (**3a**) were made using the yield ratios of $Y_{SiO_2}/Y_{Pt}/Y_{Co}$ = (1.9±0.1)/1.265/1.248 [74] and a total sputtering dose of $8{\cdot}10^{20}$ Ar ions/m^2. The sputtering yield for porous SiO_2 is not published and was determined experimentally as mentioned above. For comparison dots were fabricated using the parameters of the simulation. Results of the experiments are shown in Fig. (**3b**). The theoretical value of the dot height 11.5±1 nm deviates slightly from the experimental result 9±3 nm (Fig. **3c**). The deviation is most likely caused by different densities of the porous SiO_2 in the experiment and the calibration. To improve the accuracy it will be necessary to re-calibrate the relative sputtering yield for each batch of newly fabricated micelles. From SEM micrographs taken in normal incidence geometry (Fig. **4a**, **b**) we can determine the diameter of the SiO_2 cores and the nanodots utilizing a procedure explained before [66]. The size distribution of cores and the resulting nanodots are shown in Fig. (**4c**, **d**). An average diameter of 28±2 nm for the nominal 27 nm cores is found while the diameter is shrunk to 25±4 nm. The reduction of the diameter comes from the fact that the base point of Pt in Pt cannot be seen in the SEM image. Due to material contrast the lower interface between the Co- and Pt layer is visible which has a smaller diameter (see Fig. **4b**). The error margin is large because the contrast is very low. From the simulation we obtain a diameter of the lower Co interface of 26±2 nm. The simulation is helpful for the adaption of film structure and micelle size for optimal dot parameters. A general behavior is that the smaller the cores the thinner the film system has to be. This means that the layer sequence has to be adapted to the prerequisites of the research task.

The mean size and distance of the dots can be tuned by varying the core and/or shell diameter of the deposited micelles. An example is given in Fig. (**5**). The SEM micrographs show SiO_2 particles on a ferromagnetic multilayer after treatment in the oxygen plasma before ion milling. This flexibility in tuning particle and array dimensions is very advantageous as it allows to fitting different experimental prerequisites, like e.g. area filling to meet the experimental sensitivity, and addressing scientific questions, like e.g. interactions in arrays. Another very important feature of our fabrication procedure is the ability to independently tune the magnetic properties which is achieved *via* tuning the magnetic properties of film or multilayer.

RESULTS

To demonstrate the flexibility of tuning the magnetic properties we give some examples in the following. We restrict the discussion on film systems that are made from Co and Pt layers. It has to be mentioned that there is neither a general restriction to the film system nor the material that can be used to create dots. For experimental reasons we measure the Kerr rotation/ellipticity for fields oriented perpendicular/parallel to the film plane. All measurements discussed here were made at room temperature. Three systems will be discussed.

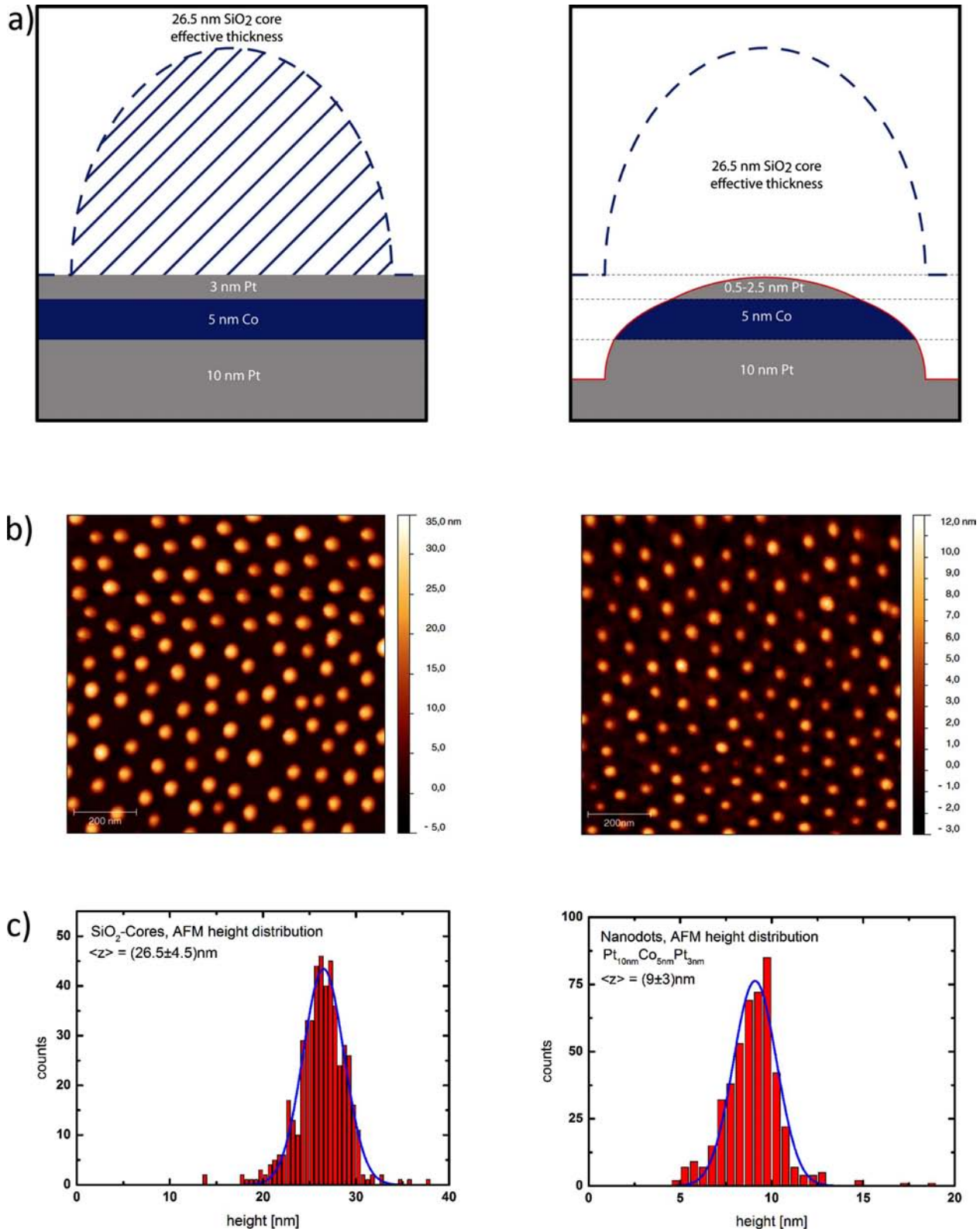

Fig. (3). (**a**) Simulation of the nanodot profile created by ion milling and experimental results. For the simulation the effective thickness of the SiO_2 core that acts as protecting shield (left-hand side) was calculated. On applying a dose of $8 \cdot 10^{20}$ Ar ions / m^2 the SiO_2 is removed and a profile in the multilayer is generated (right-hand side). For sake of simplicity a re-deposition and the angle dependence of sputter yields were not considered. Sputter yields for Pt and Co were taken from [74]. The relative yield of the porous SiO_2 compared to Pt was experimentally determined. A ratio of 1.9±0.1 has been found. (**b**) AFM measurements of the SiO_2 (left) and the dots after ion milling (right). The lower panel (**c**) shows the height distribution of the structures from (**b**). The height of the magnetic nanodots obtained from the simulation is slightly larger than the experimental value which is most likely caused by slight variation of the density of the porous SiO_2 used in the experiment and calibration.

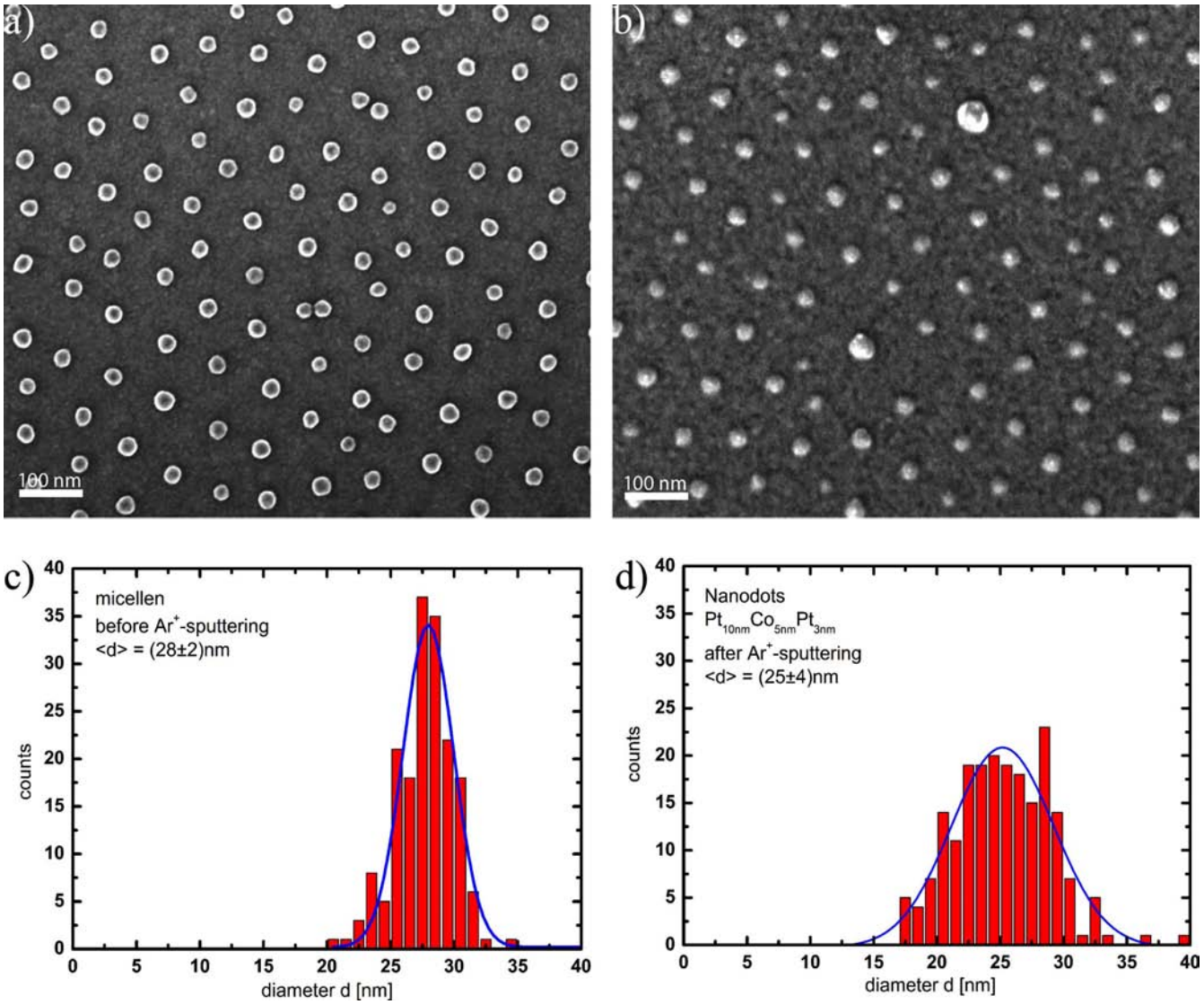

Fig. (4). SEM micrograph taken under normal incident. In (**a**) SiO_2 cores are shown before sputtering. Image (**b**) displays the magnetic dot array obtained after milling the sample shown in (**a**). The plots in (**c**, **d**) show the size distribution of the SiO_2 cores (**c**) and the nanodots (**d**) obtained by analyzing the SEM micrographs (**a**, **b**). The mean diameter of the dots is smaller than the mean diameter of the SiO_2 cores. The width of the size distribution increases after sputtering.

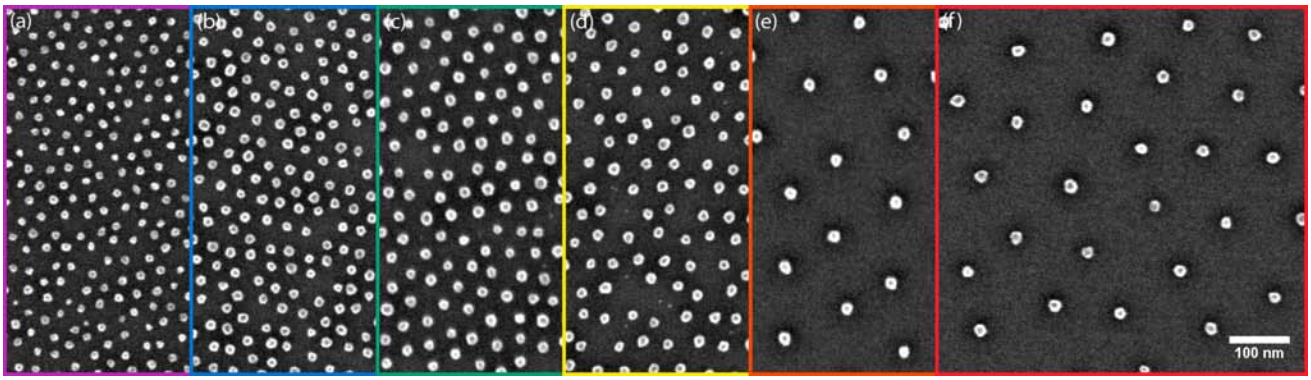

Fig. (5). SEM micrographs of samples covered by different SiO_2 cores. Nominal diameter and separation of the cores increase from left to right. With *D* the particle diameter and *a* the center to center distance, the values are: (**a**) D = 12 nm, a = 32 nm, (**b**) D = 17 nm, a = 36 nm, (**c**) D = 18 nm, a = 43 nm, (**d**) D = 18 nm, a = 48 nm, (**e**) D = 20 nm, a = 112 nm, (**f**) D = 20 nm, a = 125 nm.

1) In an earlier publication it has been demonstrated that ferromagnetic nanostructures with an easy axis of magnetization perpendicular to the surface can be fabricated [66]. The nanodots were made from a $Pt_{4.1nm}Co_{0.7nm}Pt_{2nm}Co_{0.7nm}Pt_{3nm}$ multilayer. The dot diameter was 17±2 nm. It was found that the coercivity of the dots is increased compared to the film system which was assigned to the difference of the reversal mechanisms in dots and films [66]. A multilayer of the same composition, with strong perpendicular magnetic anisotropy, has been used to create smaller dots with a diameter of 12±3 nm (separation ~30 nm). The dots exhibit a superpara-magnetic behavior (Fig. **6**). The magnetization curves for fields acting along the surface normal and parallel to the film plane are shown. Both curves have an s-like shape with no remanence. The magnetization behavior is not depending on the in-plane field orientation. Although measured at the same temperature different M(H) curves are obtained for perpendicular and in-plane oriented films (Fig. **6**) which immediately demonstrates that the magnetic anisotropy is still effective in the dots. This means that the system represents a superparamagnetic system with uniaxial behavior, similar to the results for magnetic cobalt chains on platinum [75]. In common experiments on superparamagnetism the particles are randomly oriented which eliminates any uniaxial behavior although the individual particle might behave like a uniaxial magnet. In that sense the system created here is unique as it allows the investigation of the superparamagnetic behavior with respect to distinct axes. It is possible to fit the two independent measurements (Fig. **6**) with a Boltzmann statistic for classical moments including the uniaxial magnetic anisotropy. For the fitting of both curves the same set of parameters are used (Fig. **6**) which allows us to extract an average anisotropy. We obtain for the ratio $K_1/2M_S$ = 0.1435 J/(Am) from which the first order anisotropy constant K_1 = 410 kJ/m^3 is achieved using $M_S = 1{,}44 \cdot 10^6$ A/m [76]. This value is within the estimated span of the film anisotropy which could not be determined accurately for experimental reasons.

2) The advantage of the fabrication process is that the properties of the dots can be manipulated in various ways. To tune the dot anisotropy towards an isotropic behavior a film with easy axes of magnetization within the film plane is used. The magnetization behavior of the Co film sandwiched by Pt ($Pt_{10nm}/Co_{5nm}/Pt_{3nm}$) is shown in the insets of Fig. (**7**). The M/H curve in vertical fields reveals a hard axis behavior with an anisotropy constant in the range of the shape anisotropy (inset 7a). The hysteresis obtained in fields parallel to the surface gives a magnetization curve that saturates in very small fields. A small field scan for different in-plane directions is shown in inset 7b), which reveals almost the same magnetization behavior in all measured field orientations. The latter indicates that the system behaves almost isotropic within the film plane. There is no remarkable aligning force within the film plane and the dots can be expected to reveal a superparamagnetic response within the film plane due to thermal excitations. The result of the investigation is shown in Fig. (**7**) for nanodots with a diameter of 25±4 nm (separation ~94 nm). As expected the behavior in-plane has changed from the step like response to an s-like magnetization curve. Surprisingly, a strong response is also found in vertical field. This is due to the reduced lateral size of

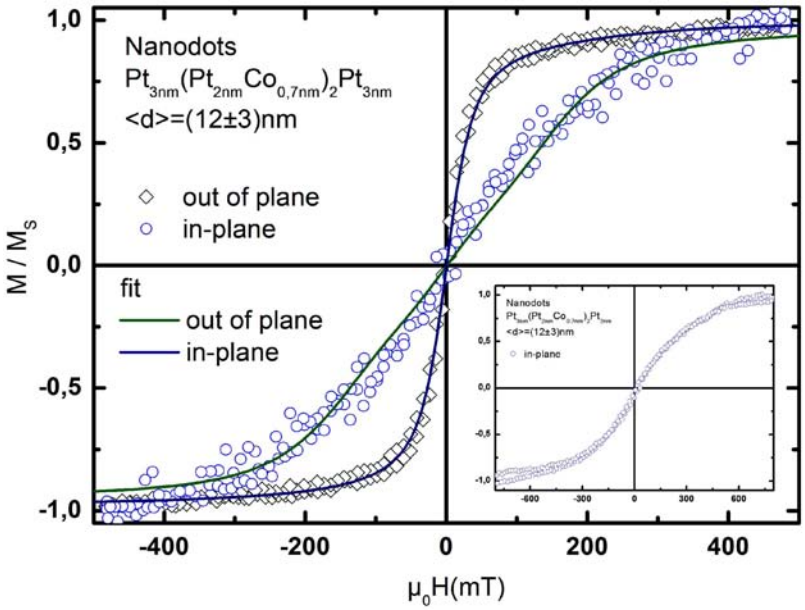

Fig. (6). Magnetization behavior of nanodots. The dots consist of $Pt_{4.1nm}Co_{0.7nm}Pt_{2nm}Co_{0.7nm}Pt_{3nm}$ with a mean diameter of 12 nm (separation~94 nm). The two curves display the Kerr ellipticity/rotation obtained in in-plane/perpendicular fields, respectively. The nanodot ensemble exhibits a superparamagnetic behavior with an easy axis perpendicular to the plane. The inset shows the magnetization behavior of the dots in higher field applied parallel to the film surface. The system still cannot be saturated as expected for superparamagnetic behavior.

the dots. Calculating the shape, assuming a disk like dot [77], we obtain a reduction of the shape anisotropy by a factor of two. This brings the effective shape anisotropy into the range of the first order bulk anisotropy of hcp Co (0,5 MJ/m^3 [76]). Both remaining anisotropies favor contrary alignment (in-plane or perpendicular, respectively). As a consequence they almost compensate and the remaining effective anisotropy is very small. An almost isotropic superparamagnetic behavior reveals although the dot morphology is by no means spherical. This example demonstrates that in Co dots, due to the strong magneto crystalline anisotropy, the dot shape manifests already in the hysteresis for particles with a ratio of diameter to thickness of about 5. The conclusion is that solely *via* the thickness of cobalt the properties of the dots can be tuned to ferromagnetism or different superparamagnetic behavior, i.e. to anisotropic as well as isotropic behavior.

3) The fabrication of layered systems gives another opportunity to vary magnetic quantities of the dots. Besides the tuning of the magnetic anisotropy it is possible when changing to multilayers to vary independently magnetic anisotropy and magnetic volume. The latter flexibility allows for setting e.g. the blocking temperature on purpose. An example is given in which about the same size of nanodots but a multilayer of much smaller total Co thickness with perpendicular anisotropy ($Pt_{4nm}(Pt_{2nm}Co_{0.8nm})_2Pt_{3nm}$) is used. Fig. (**8**) gives the magnetization curves for two different dot arrays made from the same multilayer with first order anisotropy of $K_{1,eff}$ = 47 kJ/m^3. The diameter of the magnetic dots is 22±3 nm and 26±4 nm, respectively (separation ~115 nm/102 nm). Both curves are attained in vertical fields. Although the starting magnetic anisotropy is considerably higher in the multilayer the hysteresis curves look very similar compared to those shown in Fig. (**7**). This comes from the reduced magnetic volume which is also evidenced by the strong change of magnetic behavior on the reduction of the diameter by 10%. The smaller diameter should increase the perpendicular anisotropy due to shape effects (example above) and support the anisotropic behavior. The volume reduction, however, over-compensates the latter effect and the magnetic behavior of the dot is more determined by the thermal activation. The dots are obviously very close to the blocking temperature. For the larger dots the blocking temperature is closer to room temperature than for the smaller dots.

CONCLUSION

It is shown that mask replication of periodic structures into films *via* ion etching is a versatile technique for the fabrication of nanodots that allows the tuning of various parameters. Nanodot arrays with different properties have been generated, characterized and discussed in this paper. It is demonstrated that the separation of nano-structuring and the processes determining the magnetic properties is the key advantage. It allows the fabrication of nanodots out of almost any magnetic thin film system. The main ingredients are the availability of nanosized elements that can be deposited on the film as array of well separated elements and a mild ion milling that does not strongly affect the magnetic properties. This procedure gives the researcher the high flexibility that is needed to address different scientific questions.

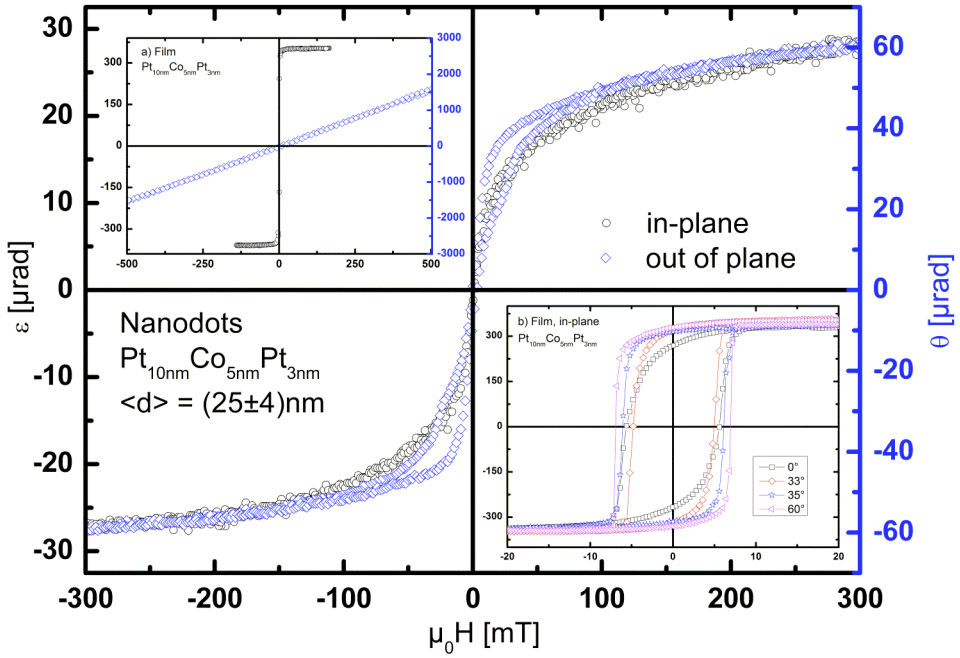

Fig. (7). Magnetization behavior of nanodots made from a magnetic film with easy plane (film plane) behavior. The dots have a diameter 25±4 nm (see also histogram in Fig. (**5**); separation ~94 nm). The response within the film plane and perpendicular to the film is very similar. The lateral structuring drastically reduces the shape anisotropy that dominates the film property. The inset a) displays the magnetization response of the corresponding film. The inset b) shows the in-plane response in small fields for different field orientations.

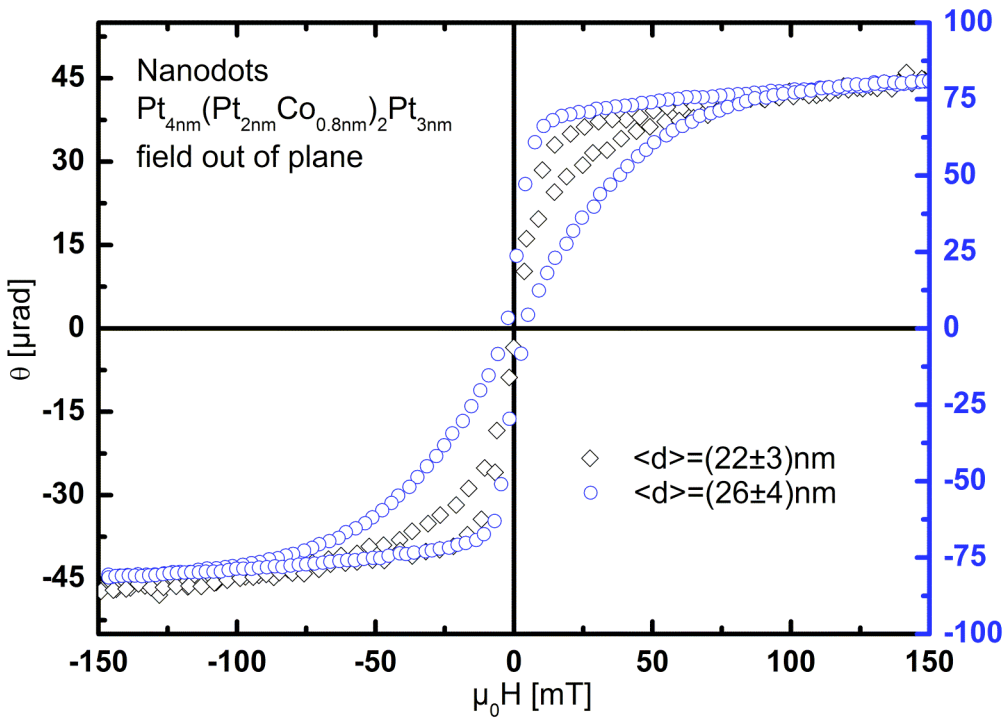

Fig. (8). Magnetization behavior of nanodots in perpendicular fields (perpendicular to the substrate surface). The two types of nanodots were fabricated from the same film system utilizing different SiO_2 cores. The diameter of the nanodots is 22±3 nm and 26±4 nm (separation ~115 nm/102 nm).

ACKNOWLEDGEMENT

Financial support by the DFG *via* SFB668 and the Free and Hanseatic City of Hamburg *via* Landesexzellenzinitative "Nanospintronics" is gratefully acknowledged.

CONFLICT OF INTEREST

The authors confirm that this article content has no conflicts of interest.

REFERENCES

[1] Nötzel R, Temmyo J, Tamamura T. Self-organized growth of strained InGaAs quantum disks. Nature 1994; 369: 131-2.

[2] Stuart HR, Hall DG. Absorption enhancement in silicon-on-insulator waveguides using metal island films. Appl Phys Lett 1996; 69: 2327-3.

[3] Bradley JS. The Chemistry of Transition Metal Colloids. In: Schmid G, Ed. Cluster and Colloids - from theory to applications. Weinheim: VCH 1994; pp. 459-544.

[4] Andres RP, Bein T, Dorogi M, *et al.* "Coulomb Staircase" at room temperature in a self-assembled Molecular Nanostructure. Science 1996; 272: 1323-2.

[5] Davidovic D, Tinkham M. Coulomb blockade and discrete energy levels in Au nanoparticles. Appl Phys Lett 1998; 73: 3959-3.

[6] Fang H, Zeller R, Stiles PJ. Fabrication of quasi-zero-dimensional submicron dot array and capacitance spectroscopy in a GaAs/AlGaAs heterostructure. Appl Phys Lett 1989; 55: 1433-3.

[7] Green M, Gracia-Parajo M, Khaleque F, Murray R. Quantum pillar structures on n+ gallium arsenide fabricated using "natural" lithography. Appl Phys Lett 1993; 62: 264-3.

[8] Bréchignac C, Houdy P, Lahmani M. Nanomaterials and Nanochemistry. Berlin: Springer 2006.

[9] Pankhurst QA, Thanh NKT, Jones SK, Dobson J. Progress in applications of magnetic nanoparticles in biomedicine. J Phys D Appl Phys 2009; 42: 224001-15.

[10] Terris BD, Thomson T. Nanofabricated and self-assembled magnetic structures as data storage media. J Phys D Appl Phys 2005; 38: R199-24.

[11] Martin JI, Nogués J, Liu K, Vicent JL, Schuller IK. Ordered magnetic nanostructures: fabrication and properties. J Magn Magn Mater 2003; 256: 449-52.

[12] Weller D, Moser A. Thermal effect limits in ultrahigh-density magnetic recording. IEEE Trans Magn 1999; 35: 4423-16.

[13] Slonczewski JC. Current-driven excitation of magnetic multilayers. J Magn Magn Mater 1996; 96: L1-7.

[14] Berger L. Emission of spin waves by a magnetic multilayer traversed by a current. Phys Rev B 1996; 54: 9353-5.

[15] Katine JA, Albert FJ, Buhrman RA. Current-driven magnetization reversal and spin-wave excitations in Co/Cu/Co pillars. Phys Rev Lett 2000; 84: 3149-3.

[16] Kiselev SI, Sankey JC, Krivorotov IN, *et al.* Microwave oscillations of a nanomagnet driven by a spin-polarized current. Nature 2003; 425: 380-3.

[17] Rippard WH, Pufall MR, Kaka S, Russek SE, Silva TJ. Direct-current induced dynamics in Co90Fe10/Ni80Fe20 point contacts. Phys Rev Lett 2004; 92: 027201-4.

[18] Schmid G, Ed. Cluster and Colloids - from theory to applications. VCH: Weinheim 1994.

[20] Sun S, Murray CB, Weller D, Folks L, Moser A. Monodisperse FePt nanoparticles and ferromagnetic FePt nanocrystal superlattices. Science 2000; 287: 1989-3.

[21] Frey NA, Peng S, Cheng K, Sun S. Magnetic nanoparticles: synthesis, functionalization, and applications in bioimaging and magnetic energy storage. Chem Soc Rev 2009; 38: 2532-10.

[22] Puntes VF, Krishnan KM, Alivisatos AP. Colloidal nanocrystal shape and size control: The case of cobalt. Science 2001; 291: 2115-2.

[23] Shevchenko EV, Talapin DV, Rogach AL, *et al.* Colloidal synthesis and self-assembly of CoPt3 nanocrystals. J Am Chem Soc 2002; 124: 11480-5.

[24] Caruso F, Schüler C. Enzyme multilayer on colloid particles: Assembly, stability, and enzymatic activity. Langmuir 2000; 16: 9595-8.

[25] Hutten A, Sudfeld D, Ennnen I, *et al*. New magnetic nanoparticles for biotechnology. J Biotechnol 2004; 112: 47-16.

[26] Torney F, Trewyn BG, Lin VS-Y, Wang K. Mesoporous silica nanoparticles deliver DNA and chemicals into plants. Nat Nanotechnol 2007; 2(5): 295-300.

[27] Gao JH, Gu HW, Xu B. Multifunctional magnetic nanoparticles: Design, synthesis, and biomedical applications. Acc Chem Res 2009; 42: 1097-10.

[28] Spatz JP, Mossmer S, Hartmann C, *et al.* Ordered deposition of inorganic clusters from micellar block copolymer films. Langmuir 2000; 16: 407-8.

[29] Antoniak C, Lindner J, Spasova M, *et al.* Enhanced orbital magnetism in Fe50Pt50 nanoparticles. Phys Rev Lett 2006; 97: 117201-4.

[30] Ethirajan A, Wiedwald U, Boyen H-G, *et al.* A micellar approach to magnetic ultrahigh-density data-storage media: extending the limits of current colloidal methods. Adv Mater 2007; 19: 406-4.

[31] Hauet T, Dobisz E, Florez S, *et al.* Role of reversal incoherency in reducing switching field and switching field distribution of exchange coupled composite bit patterned media. Appl Phys Lett 2009; 95: 262504-3.

[32] Hellwig O, Berger A, Thomson T, *et al.* Separating dipolar broadening from the intrinsic switching field distribution in perpendicular patterned media. Appl Phys Lett 2007; 90: 162516-3.

[33] Hellwig O, Hauet T, Thomson T, *et al*. Coercivity tuning in Co/Pd multilayer based bit patterned media. Appl Phys Lett 2009; 95: 232505-3.

[34] Schabes ME. Micromagnetic simulations for terabit/in² head/media systems. J Magn Magn Mater 2008; 320: 2880-4.

[35] Smith HI, Flanders DC. Oriented crystal growth on amorphous substrates using artificial surface-relief gratings. Appl Phys Lett 1978; 32: 349-2.

[36] Segalman RA, Yokoyama H, Kramer EJ. Graphoepitaxy of spherical domain block copolymer films. Adv Mater 2001; 13: 1152-3.

[37] Cheng JY, Ross CA, Thomas EL, Smith HI, Vancso GJ. Templated self-assembly of block copolymers: Effect of substrate topography. Adv Mater 2003; 15: 1599-4.

[38] Ruiz R, Kang H, Detcheverry F A, *et al.* Density multiplication and improved lithography by directed block coplolymer assembly. Science 2008; 321: 936-3.

[39] Bita I, Yang JKW, Jung YS, *et al.* Graphoepitaxy of self-assembled block copolymers on two-dimensional periodic patterned templates. Science 2008; 321: 939-4.

[40] Hellwig O, Bosworth JK, Dobisz E, *et al*. Bit patterned media based on block copolymer directed assembly with narrow magnetic switching field distribution. Appl Phys Lett 2010; 96: 052511-3.

[41] Luo F, Heyderman LJ, Solak HH, Thomson T, Best ME. Nanoscale perpendicular magnetic island arrays fabricated by extreme ultraviolet intference lithography. Appl Phys Lett 2008; 92: 102505-3.

[42] Elmers HJ, Hausschild J, Hoche H, *et al.* Submonolayer magnetism of Fe(110) on W(110) – Finite-width scaling of stripes and percolation between islands. Phys Rev Lett 1994; 73: 898-3.

[43] Pietzsch O, Okatov S, Kubtezka A, *et al.* Spin resolved electronic structure of nanoscale cobalt islands on Cu(111). Phys Rev Lett 2006; 96: 237203-4.

[44] Prokop J, Kukunin A, Elmers HJ. Spin-polarized scanning tunneling microscopy and spectroscopy of ultrathin Fe/Mo(110) films using W/Au/Co tips. Phys Rev B 2006; 73: 014428-7.

[45] Wasniowska M, Wulfhekel W, Przybylski M, Kirschner J. Submonolayer regime of Co epitaxy on Pd(111): Morphology and electronic structure. Phys Rev B 2008; 78: 035405-8.

[46] Rodary G, Wedekin S, Sander D, Kirschner J. Magnetic hysteresis loop of single Co nano-islands. Jpn J Appl Phys 2008; 47: 9013-2.

[47] Teichert C, Bartel J, Oepen HP, Kirschner J. Fabrication of nanomagnet arrays by shadow deposition on self-organized semiconductor substrates. Appl Phys Lett 1999; 74: 588-3.

[48] Facsko S, Dekorsy T, Koerdt C, *et al.* Formation of ordered nanoscale semiconductor dots by ion sputtering. Science 1999; 285: 1551-2.

[49] Thrun-Albrecht T, Schotter J, Kästle G A, *et al.* Ultrahigh-density nanowire arrays grown in self-assembled diblock copolymer templates. Science 2000; 290: 2126-3.

[50] Krausch G, Magerle R. Nanostructured thin films *via* self-assembly of block copolymers. Adv Mater 2002; 14: 1579-4.

[51] Park C, Yoon J, Thomas EL. Enabling nanotechnology with self-assembled block copolymer patterns. Polymere 2003; 44: 6725-35.

[52] Cheng JY, Jung W, Ross CA. Magnetic nanostructures from block copolymer lithography: Hysteresis, thermal stability, and magnetoresistance. Phys Rev B 2004; 70: 064417-9.

[53] Ross CA. Patterned magnetic recording media. Ann Rev Mater Res 2001; 31: 203-32.

[54] Ross CA, Cheng JY. Patterned magnetic media made by self-assembled block-copolymer lithography. MRS Bull 2008; 33: 838-7.

[55] Deckman HW, Dunsmuir JH. Natural lithography. Appl Phys Lett 1982; 41: 377-2.

[56] Hulteen JC, Vanduyne RP. Nanosphere lithography – A materials general fabrication process for periodic particle array surfaces. J Vac Sci Technol A 1995; 13: 1553-5.

[57] Albrecht M, Hu G, Guhr IL, *et al.* Magnetic multilayers on nanospheres. Nat Mater 2005; 4: 203-3.

[58] Choi DG, Kim S, Jang S-G, *et al.* Nanopatterned magnetic metal *via* colloidal lithography with reactive ion etching. Chem Mater 2004; 16: 4208-3.

[59] Li X, Tadisina ZR, Gupta S, Ju GP. Preparation and properties of perpendicular CoPt magnetic nanodot arrays patterned by nanosphere lithography. J Vac Sci Technol A 2009; 27: 1062-4.

[60] Haginoya C, Ishibashi M, Koike K. Nanostructure array fabrication with a size-controllable natural lithography. Appl Phys Lett 1997; 71: 2934-2.

[61] Huang Z, Fang H, Zhu J. Fabrication of silicon nanowire arrays with controlled diameter, length and density. Adv Mater 2006; 19: 744-5.

[62] Plettl A, Enderle F, Saitner M, *et al.* Non-close-packed crystals from self-assembled polystyrene spheres by isotropic plasma etching: Adding flexibility to colloid lithography. Adv Funct Mater 2009; 19: 3279-5.

[63] Wenig C-C, Hsu K-F, Wie K-H. Synthesis of arrayed, TiO2 needlelike nanostructures *via* a polystrene-block-poly(4-vinylpyridine) diblock Copolymer template. Chem Mater 2004; 16: 4080-6.

[64] Sun Z, Wolkenhauer M, Bumbu G-G, Gutmann DH, Kim JS. GISAXS investigation of TiO2 nanoparticles in PS-b-PEO block-copolymer films. Physica B 2005; 357: 141-2.

[65] Frömsdorf A, Kornowski A, Pütter S, Stillrich H, Lee LT. Highly ordered nanostructured surfaces obtained with silica-filled diblock-copolymer micelles as templates. Small 2007; 3: 880-10.

[66] Stillrich H, Frömsdorf A, Förster S, Pütter S, Oepen HP. Sub-20 nm magnetic dots with perpendicular magnetic anisotropy. Adv Funct Mater 2008; 18: 76-5.

[67] Wellhöfer M, Weissenborn M, Anton R, Pütter S, Oepen HP. Morphology and magnetic properties of ECR ion beam sputtered Co/Pt films. J Magn Magn Mater 2005; 292: 345-13.

[68] Stillrich H, Menk C, Frömter R, Oepen HP. Magnetic anisotropy and the cone state in Co/Pt multilayer films. J Appl Phys 2009; 105: 07C308-3.

[69] Förster S, Zisenis M, Wenz E, Antonietti M. Micellization of strongly segregated block copolymers. J Chem Phys 1996; 104: 9956-15.

[70] Gästle G, Boyen HG, Weigl F, *et al.* Micellar nanoreactors – Preparation and characterization of hexagonally ordered arrays of metallic nanodots. Adv Funct Mater 2003; 13: 853-8.

[71] Wagner A, Levin JP, Mauer JL, *et al.* X-ray mask repair with focused ion beams. J Vac Sci Technol B 1990; 8: 1557-7.

[72] Mayer J, Giannuzzi LA, Kamino T, Micheal J. TEM sample preparation and FIB-induced damage. MRS Bull 2007; 32: 400-7.

[73] Stark Y, Frömter R, Stickler D, Oepen HP. Sputter yields of single- and polycrystalline metals for application in focused ion beam technology. J Appl Phys 2009; 105: 013542-5.

[74] npl.co.uk. Teddington: National Physical Laboratory; c2005-12 [updated: 27th May 2005]. Ar Sputtering Yields at 0°;[one page]. Available from: http://www.npl.co.uk/science-technology/surface-and-nanoanalysis/services/sputter-yield-values [Cited: 15th February 2011]

[75] Gambardella P, Dallmeyer A, Maiti K, *et al.* Oscillatory magnetic anisotropy in one-dimensional atomic wires. Phys Rev Lett 2004; 93: 077203-4.

[76] Stearns MB. Landolt-Börnstein: Group III. Berlin: Springer 1986; Vol 19a.

[77] Millev YT, Vedmedenko E, Oepen HP. Dipolar magnetic anisotropy energy of laterally confined ultrathin ferromagnets: multiplicative separation of discrete and continuum contributions. J Phys D Appl Phys 2003; 36: 2945-4.

Received: May 26, 2011 Revised: March 14, 2012 Accepted: March 15, 2012